

# Journal of Biomedical Optics

BiomedicalOptics.SPIEDigitalLibrary.org

## **Imaging autofluorescence temporal signatures of the human ocular fundus *in vivo***

Asael Papour  
Zachary Taylor  
Oscar Stafsudd  
Irena Tsui  
Warren Grundfest

# Imaging autofluorescence temporal signatures of the human ocular fundus *in vivo*

Asael Papour,<sup>a,\*</sup> Zachary Taylor,<sup>b</sup> Oscar Stafsudd,<sup>a</sup> Irena Tsui,<sup>c</sup> and Warren Grundfest<sup>b</sup>

<sup>a</sup>University of California, Los Angeles, Electrical Engineering Department, 56-125B Engineering, IV Building, 420 Westwood Plaza, Los Angeles, California 90095-1594, United States

<sup>b</sup>University of California, Los Angeles, Department of Bioengineering, 410 Westwood Plaza, Room 5121, Engineering V, P.O. Box 951600, Los Angeles, California 90095-1600, United States

<sup>c</sup>University of California, Los Angeles, Stein Eye Institute and Doheny Eye Institute, 100 Stein Plaza, Los Angeles, California 90095-7000, United States

**Abstract.** We demonstrate real-time *in vivo* fundus imaging capabilities of our fluorescence lifetime imaging technology for the first time. This implementation of lifetime imaging uses light emitting diodes to capture full-field images capable of showing direct tissue contrast without executing curve fitting or lifetime calculations. Preliminary results of fundus images are presented, investigating autofluorescence imaging potential of various retina biomarkers for early detection of macular diseases. © 2015 Society of Photo-Optical Instrumentation Engineers (SPIE) [DOI: [10.1117/1.JBO.20.11.110505](https://doi.org/10.1117/1.JBO.20.11.110505)]

**Keywords:** fluorescence lifetime imaging microscopy; real-time imaging; retina.

Paper 150185LRRR received Mar. 20, 2015; accepted for publication Oct. 22, 2015; published online Nov. 23, 2015.

Fluorescence lifetime imaging microscopy is a robust imaging modality that has been proven to be sensitive in the detection of chemicals and molecular species in the cluttered environments.<sup>1-3</sup> The examples specific to biomedical imaging are the detection of cancerous tumors<sup>4,5</sup> and metabolic changes in the human fundus, aimed to characterize and provide better disease prognosis. Research efforts in the field reported various fluorescence biomarkers and structural contrast mechanisms to investigate detection capabilities for age-related macular degeneration (AMD), diabetic retinopathy, etc.<sup>6-12</sup> These systems utilize point detection by raster scanning and result in long acquisition and processing times. Our group has developed a new imaging method utilizing autofluorescence temporal signatures to test the efficacy of a direct image contrast in various tissues. This technique does not require setting *a priori* assumptions on the fluorescence decay behavior and displays a contrast map based on relative changes in lifetime (Fig. 1). The contrast

image can be acquired and processed in less than a second.<sup>5,13,14</sup> In this letter, we demonstrate the system's capability in imaging full-field human fundus with low-excitation fluence and show structural variations *in vivo*.

## 1 System and Methods

The illumination scheme in the system relies on a wide-field illumination by a diffused light emitting diode (LED) light providing excitation at 407 nm. Using this wavelength in imaging, the retina is possible in pseudophakic patients, as the intraocular lens efficiently transmits blue wavelengths and assists in reducing the autofluorescence signal found in crystalline lenses.<sup>15,16</sup> Blue wavelengths have also been reported to efficiently excite metabolic fluorophores such as flavin adenine dinucleotide and lipofuscin, among other fluorophores in the retina and pigment epithelium, with strong signals from structural fluorophores, collagen, and elastin.<sup>12,17-19</sup> These signals exhibit a broad fluorescence emission spectrum that can be imaged using our detection scheme and potentially used to detect structural and metabolic changes in the retina. The system was built on an existing fundus camera (Zeiss, FF4), which uses conventional optics (not confocal) with an indirect illumination scheme to record color images and fluorescein angiographs from a human retina. Modifications were made to enable imaging of the retina's autofluorescence signals (Fig. 2) and include an intensified CCD (ICCD) imager (Andor, iStar 334T) and an LED (Thorlabs, LED405E) set to emit 20-ns long square pulses with 407-nm wavelength and average power of 4  $\mu$ W at the cornea. Utilizing a blue wavelength with low power levels and flat-top pulses with low average and peak power has been found safe both by the ANSI standard for ocular exposure<sup>20,21</sup> and reported DNA-damage threshold statistics.<sup>22</sup> The LED light passes through two ultraviolet (UV) optical filters (Thorlabs, FEL0400) to ensure no residual UV light reaches the imaged eye. Another filter is positioned in front of the ICCD to block reflected light and record fluorescence signals from the retina at a central wavelength of 460- and 60-nm bandwidth (Semrock, FF01-460/60-25). A high-power pulse generator (Avtech, AVR-E3-B-P) drives the LED and triggers the camera operation. The relatively low duty cycle (<0.2%) and the LED impedance matching network ensure optical output without damaging the LED and maintain wavelength stability for extended periods.

## 2 Results and Discussion

*Ex vivo* porcine eyes were used as a calibration model for the camera before *in vivo* experiments were performed, as they exhibit similar properties to the human eye. Six fresh eyes, kept in ice to slow tissue deterioration and delivered within 2 h of harvesting, were acquired from a local slaughterhouse in adherence to the Association for Research in Vision and Ophthalmology statement for the use of animals in ophthalmic and vision research. No Institutional Review Board approval was required. The chosen excitation wavelength transmits through the intraocular structures, i.e., lens and vitreous, and excites the retina and blood vessels (Fig. 3).

All of the porcine eyes resulted in low-detail images due to various degrees of corneal edema (high hydration levels that cause opaqueness). Contrast in these images originates primarily from the lifetime difference between blood vessels and

\*Address all correspondence to: Asael Papour, E-mail: [papour@ucla.edu](mailto:papour@ucla.edu)

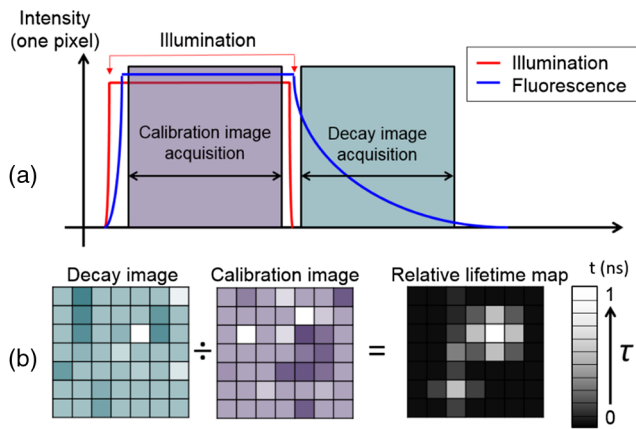


**Fig. 1** The relative fluorescent lifetime algorithm introduces both hardware and software modifications to the fluorescence lifetime imaging microscopy modality to produce a contrast image: (a) acquisition of only two images is necessary; one during illumination (calibration image) and the second during fluorescence decay (decay image). Each image is acquired by the accumulation of many repetitive pulses by the gated camera to achieve adequate signal level. (b) The decay image is divided by the calibration image using pixel division and results in a final relative (normalized) lifetime image. High signal levels can be achieved, since the fluorescence intensity is recorded over a relatively long acquisition period (10 to 20 ns) and with good camera-gating efficiency (>90%). Since the fluorophore lifetime and recorded signals are correlated, this algorithm produces lifetime contrast information without depending on yield or concentration factors.

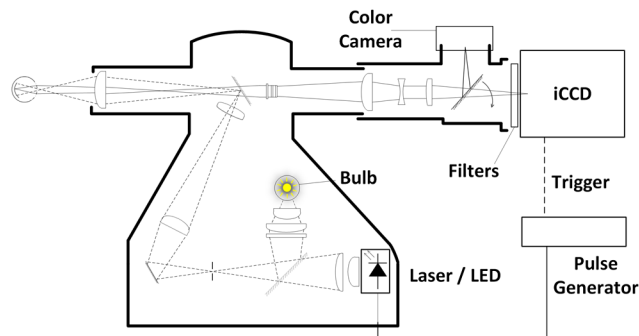


**Fig. 2** Modified fundus camera schematics: light emitting diode (LED) and an intensified CCD (iCCD) are set to generate and capture nano-second autofluorescence signals from the retina. The LED replaces a xenon flash bulb and the iCCD replaces a conventional CCD module; both were used in traditional angiography procedures. Images captured by pulsing the LED and synchronizing the iCCD by the pulse generator. The iCCD is capable of intensifying and imaging the signals to provide full-field images without raster scanning in real time.

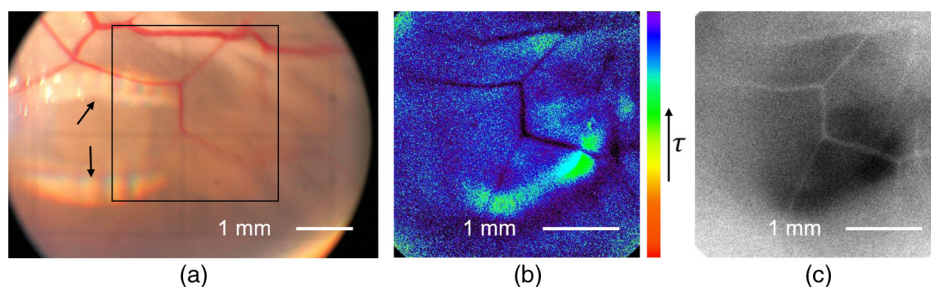


**Fig. 3** *Ex vivo* porcine eye imaging using fundus camera. (a) Color fundus image, square represents field of view of the fluorescence images, and black arrows point at reflections. (b) Color threshold autofluorescence relative lifetime image. (c) Gray-scale threshold autofluorescence relative lifetime contrast image.

retinal connective tissue fluorophores, collagen, and elastin. The contribution of the lens' strong autofluorescence signal could explain variations in contrast.<sup>17</sup>

The *in vivo* imaging experiment included six pseudophakic volunteer patients from the Stein Eye Institute at University of California, Los Angeles. The experiment was approved by the Internal Review Board for human subjects. Three out of the six patients were imaged successfully during system optimization and operator training. Two of the patients were diagnosed with dry AMD [Figs. 4(a)–4(c) and 4(g)–4(i)] and one patient with diabetic retinopathy [Figs. 4(d)–4(f)]. Images of the diabetic patient show low signal levels and bright spots (hyperfluorescence) of macular edema.<sup>23</sup> The fluorescence intensity map shows better contrast than the lifetime data, and more data are needed in order to validate possible imaging utility for this condition. The first AMD patient [Figs. 4(a)–4(c)] displays high noise level, though the basic lifetime contrast between the optic disk and the surrounding retina is visible. Figures 4(b) and 4(c) were taken at different times. Images of the second AMD patient [Figs. 4(g)–4(i)] exhibit higher detail level and contrast due to optics optimizations. The lifetime image [Fig. 4(h)] shows signals of the optic disk and blood vessels' margins generated mainly from connective tissue fluorophores. Longer lifetime values in the fovea region are also visible and correlate to previously reported lifetime changes in AMD patients.<sup>24</sup> However, more patient data are needed in order to demonstrate reproducibility and statistical significance. The current fundus camera was not designed for lifetime imaging and has low photon efficiency, though basic fluorescence lifetime data displayed show the robustness of the technique. Diagnosis of AMD, specifically lipofuscin distribution, could possibly be achieved with a modern fundus imager that has higher photon efficiency and reduced reflections.

### 3 Conclusions

We have shown a proof of concept of our technique in imaging retina autofluorescence lifetime signatures. Implementation of this imaging method on a modern fundus camera could offer an alternative to existing technologies, using fast fundus imaging without raster scanning. Further improvement of the illumination pulse profile and algorithm optimizations could extract more information and increase signal-to-noise ratio. Implementation of multispectral excitation schemes in future research efforts could also provide better discrimination and contrast of endogenous fluorophores to detect metabolic processes and morphological changes in point of care macular diagnosis.

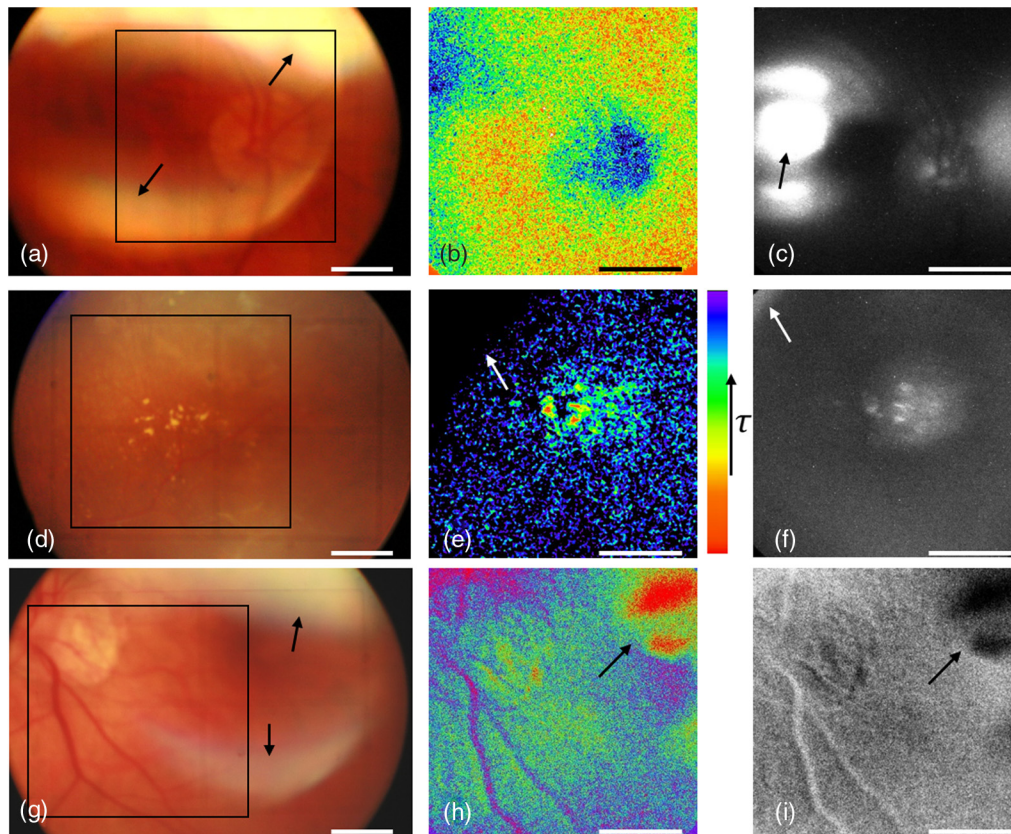


**Fig. 4** Color fundus photos of three patients, and individual color threshold was set for each image to enhance contrast. Each row represents a single eye measurement, and squares in (a), (d) and (g) represent the field of view of the fluorescence images. (b), (e), and (h) are fluorescence lifetime contrast images, (c), (f), and (i) are fluorescence gray-scale intensity images. Arrows point at reflections artifacts (common in pseudophakic patients). Images (c) and (b) taken at different times [image (b) has no reflection artifact]. Scale bars in all images are 1 mm.

### Acknowledgments

This work was sponsored by the Telemedicine and Advanced Technology Research Center, Grant No. W81XWH-12-2-0075. Support of this study was provided by the Stein Eye Institute by donation of equipment. Imaging of patients was approved by University of California, Los Angeles Institutional Review Board, IRB 14-000767.

### References

1. N. Mazumder et al., "Fluorescence lifetime imaging of alterations to cellular metabolism by domain 2 of the hepatitis C virus core protein," *PLoS One* **8**(6), e66738 (2013).
2. T. S. Blacker et al., "Separating NADH and NADPH fluorescence in live cells and tissues using FLIM," *Nat. Commun.* **5**, 3936 (2014).
3. J.-M. I. Maarek et al., "Time-resolved fluorescence spectra of arterial fluorescent compounds: reconstruction with the Laguerre expansion technique," *Photochem. Photobiol.* **71**(2), 178–187 (2000).
4. Y. Sun et al., "Fluorescence lifetime imaging microscopy for brain tumor image-guided surgery," *J. Biomed. Opt.* **15**(5), 056022 (2010).
5. A. Papour et al., "Optical imaging for brain tissue characterization using relative fluorescence lifetime imaging," *J. Biomed. Opt.* **18**(6), 060504 (2013).
6. M. Hammer et al., "In vivo and in vitro investigations of retinal fluorophores in age-related macular degeneration by fluorescence lifetime imaging," *Proc. SPIE* **7183**, 71832S (2009).
7. D. Schweitzer et al., "Fluorescence lifetime imaging ophthalmoscopy in type 2 diabetic patients who have no signs of diabetic retinopathy," *J. Biomed. Opt.* **20**(6), 061106 (2015).
8. C. Dysli, S. Wolf, and M. S. Zinkernagel, "Fluorescence lifetime imaging in retinal artery occlusion," *Invest. Ophthalmol. Vis. Sci.* **56**(5), 3329 (2015).
9. C. Dysli et al., "Quantitative analysis of fluorescence lifetime measurements of the macula using the fluorescence lifetime imaging ophthalmoscope in healthy subjects," *Invest. Ophthalmol. Vis. Sci.* **55**(4), 2106–2113 (2014).
10. A. von Rückmann, F. W. Fitzke, and A. C. Bird, "Fundus autofluorescence in age-related macular disease imaged with a laser scanning ophthalmoscope," *Invest. Ophthalmol. Vis. Sci.* **38**(2), 478–486 (1997).
11. D. Schweitzer et al., "Evaluation of time-resolved autofluorescence images of the ocular fundus," *Proc. SPIE* **5141**, 8–17 (2003).
12. M. Islam et al., "pH dependence of the fluorescence lifetime of FAD in solution and in cells," *Int. J. Mol. Sci.* **14**(1), 1952–1963 (2013).
13. P.-C. Jiang, W. S. Grundfest, and O. M. Stafsudd, "Quasi-real-time fluorescence imaging with lifetime dependent contrast," *J. Biomed. Opt.* **16**(8), 086001 (2011).
14. A. J. Sherman et al., "Normalized fluorescence lifetime imaging for tumor identification and margin delineation," *Proc. SPIE* **8572**, 85721H (2013).
15. J. A. Zuclich et al., "Near-UV/blue light-induced fluorescence in the human lens: potential interference with visual function," *J. Biomed. Opt.* **10**(4), 044021 (2005).
16. E. A. Boettner and J. R. Wolter, "Transmission of the ocular media," *Invest. Ophthalmol. Vis. Sci.* **1**(6), 776–783 (1962).
17. D. Schweitzer et al., "Spectral and time-resolved studies on ocular structures," *Proc. SPIE* **6628**, 662807 (2007).
18. A. D. Marmorstein et al., "Spectral profiling of autofluorescence associated with lipofuscin, bruch's membrane, and sub-RPE deposits in normal and AMD eyes," *Invest. Ophthalmol. Vis. Sci.* **43**(7), 2435–2441 (2002).

19. J. R. Sparrow et al., "A2E, a lipofuscin fluorophore, in human retinal pigmented epithelial cells in culture," *Invest. Ophthalmol. Vis. Sci.* **40**(12), 2988–2995 (1999).
20. *American National Standard for the Safe Use of Laser*, ANSI Z 136.1-2007, Laser Institute of America, Orlando, Florida (2007).
21. F. C. Delori, R. H. Webb, and D. H. Sliney, "Maximum permissible exposures for ocular safety (ANSI 2000), with emphasis on ophthalmic devices," *J. Opt. Soc. Am. A* **24**(5), 1250–1265 (2007).
22. R. P. Sinha and D. P. Häder, "UV-induced DNA damage and repair: a review," *Photochem. Photobiol. Sci.* **1**(4), 225–236 (2002).
23. A. Pece et al., "Autofluorescence imaging of cystoid macular edema in diabetic retinopathy," *Ophthalmologica* **224**(4), 230–235 (2010).
24. D. Schweitzer et al., "In vivo measurement of time-resolved autofluorescence at the human fundus," *J. Biomed. Opt.* **9**(6), 1214–1222 (2004).